PHYSICAL REVIEW A VOLUME 39, NUMBER 3 FEBRUARY 1, 1989

# Quenching of low-lying Rydberg states of Na colliding with ground-state He: A semiclassical approach

A. Kumar* and N. F. Lane
*Department of Physics, Rice Quantum Institute, Rice University, Houston, Texas 77251*

M. Kimura
*Argonne National Laboratory, Argonne, Illinois 60439 and Department of Physics, Rice University, Houston, Texas 77251*
(Received 9 May 1988; revised manuscript received 25 August 1988)

The molecular expansion method within the framework of the semiclassical approximation is applied to quenching of low-lying excited states of Rydberg atoms colliding with ground-state He at thermal energies. Interactions between the colliding atoms are accounted for in terms of pseudopotentials, and their relative motion is described by a classical linear trajectory. A fairly large basis set of Slater-type orbitals is used to obtain molecular eigenstates, and subsequently a 14-state close-coupling calculation is performed to evaluate the total quenching cross sections and the contributions of individual transitions. The energy dependence of the calculated cross sections is investigated, and possible mechanisms responsible for individual transitions are explained. Finally, the collision rates are calculated and compared with experimental results.

## I. INTRODUCTION

The development of tunable dye lasers and advanced techniques of high-resolution spectroscopy have made possible the selective excitation and detection of Rydberg states.[1] These advances, in turn, have led to a large number of experimental and theoretical investigations of $l$-mixing ($\Delta l$) and $n$-changing ($\Delta n$) collisions between alkali Rydberg atoms and other neutral species.[2] Moreover, the practical application of knowledge about these processes, particularly in the field of low-temperature plasmas, gas discharges, gas and flame lasers, astrophysics, etc. has also stimulated interest in their study. Theoretical investigations of Rydberg atoms interacting with neutral atoms have been based largely on the so-called "free-electron model." This model, originally proposed by Fermi,[3] takes advantage of the fact that the Rydberg electron is very weakly bound to the core and hence behaves nearly as if it were free. It is the short-range interaction of this quasifree electron with the neutral perturber that plays the decisive role in such collisions. Thus the cross sections for Rydberg atom-atom collisions often can be well described in terms of the electron-perturber scattering amplitude. This free-electron model, implemented within the framework of various other approximations, is found to give a satisfactory account of $l$-mixing cross sections for thermal-energy collisions of atoms having large principal quantum numbers. However, there are quite a number of experimental measurements on quenching ($n$ changing) that do not lend themselves to this simple treatment and that have never been subjected to rigorous theoretical investigation.[4] Of particular interest are Rydberg levels of alkali atoms for which the initial orbital angular momentum is low (for example, $s$ states for Na; $s$ and $p$ states for K; and $s$, $p$, and $d$ states for Rb). The electronic energies $E(R)$ of molecular states involved in such collisions often change substantially with internuclear distance, so that two states that have quite different energies at infinite separation may undergo curve crossings or avoided crossings [i.e., very small energy defect $\Delta E(R)$ at a finite $R$ value[5]]. When the energy defect $\Delta E(R)$ between two states is large compared with the reciprocal of the effective collision time, then the probability of a transition between the two is small. Except for special circumstances, this is the case for states having different principal quantum number $n$. Consequently the cross sections for $\Delta n$ collisions are generally much smaller than those for $l$-mixing ($\Delta l$) processes; this is always true for large initial $l$. The detailed nature of the relevant energy defects depends on core penetration of the Rydberg electron, making the applicability of the free-electron model highly questionable, particularly for intermediate-$n$ states. Of course for low-$n$ states, the model is known to fail.[6]

These considerations and the availability of experimental data motivated us to make a detailed theoretical investigation of $n$ changing in collisions of low-lying excited Na($ns$) atoms with ground-state He at thermal energies. The quantum defects for $s$ and $p$ states of Na are 1.35 and 0.85, respectively, whereas those for higher angular momenta ($l \geq 2$) are nearly zero.[7] Except for isolated avoided crossings, the adiabatic energy curves are well separated from adjacent curves, thus leading to very small quenching cross sections. Gallagher and Cooke[4] have experimentally investigated quenching of a Na($ns$) colliding with a ground-state He atom at $T=425$ K. Although only the total depopulation cross sections of the initial state have been measured, these authors have reported that for initial $n \geq 9$ both downward ($\Delta n < 0$) and upward ($\Delta n > 0$) transitions are important, whereas for $n \leq 8$, the downward transitions dominate. Thus we have studied the relative magnitudes of the respective probabilities of transition to different levels from the initial $ns$ level. We have also examined the dependence of these cross sections on relative collision velocity. Since an in-

 

crease in the principal quantum number $n$ of the Rydberg atom brings the adjacent energy levels closer to one another, it follows that for high $n$, even small changes in velocity in the thermal-energy region may lead to significant changes in the cross sections. Finally, for states of very high $n$, the relevant energy defects, even for quenching, become negligible, and the measured cross sections are found to be nearly energy independent. As detailed experimental investigations are very difficult and since most of the experimental measurements provide only the total quenching cross sections, giving little information about details of the collision dynamics, it is felt desirable to have a rigorous theoretical investigation of such processes.

There have been only a few theoretical calculations of cross sections for quenching of Rydberg atoms. Sato and Matsuzawa[8] as well as Petitjean and Gounand[9] (see also de Prunele and Pascale,[6] Omont,[10] and Derouard and Lombardi[11]) have developed simplified expressions for quenching cross sections within the framework of the impulse approximation by making use of the free-electron model. However, these calculations are valid only for very high values of the principal quantum number and lose their reliability at low $n$, where the effective energy defect for quenching is large. Indeed, de Prunele and Pascale[6] have pointed out that for low-lying Rydberg levels the theory should include the complete three-body interactions. Lebedev and Marchenko,[12] who used the Fermi pseudopotential model, and Kaulakys[13,14] have attempted to explain these collisions using a binary-encounter method. These authors obtain simplified analytical expressions for the total quenching cross sections, which they claim to be in agreement with experimental measurements performed on the Na($ns$)+He systems for $n > 10$. These calculations describe only the total depopulation of the initial state.

In contrast to the binary-encounter studies, the present method takes into account all interactions between the colliding particles at all stages of the collision event, enabling us to look into details of collision dynamics. For this we use, in the framework of semiclassical approximation, a molecular state expansion method where the electron translation factor (ETF) is fully accounted for.[15] Such methods have been successfully used in the past to investigate a variety of heavy-particle collisions.[16,17] Inclusion of the ETF accounts for the motion of the reference position for the electron with respect to the center of mass of the system. Its neglect from the molecular orbital (MO) expansion introduces spurious long-range coupling and cross sections that depend on the choice of origin. The importance of the ETF in the MO expansion method has been emphasized in Ref. 5. It may here be noted that a similar study has earlier been carried out by Valiron *et al.*[18] where two- and three-channel calculations were performed to account for population transfer of Na($6p$) colliding with He and Ne in the thermal-energy region.

Section II contains a brief description, including only essential features of the theoretical method. In Sec. III our results are presented and compared with experimental measurements. Specific mechanisms that control particular transitions are discussed. Section IV contains a summary of our observations. Throughout this paper atomic units ($e=m=a_0=\hbar=1$) are used unless otherwise stated.

## II. THEORETICAL METHOD

The standard, semiclassical impact-parameter method using a molecular expansion incorporating an ETF has been used in the present investigation. Since the Na-He system can be adequately represented by one electron loosely bound to the ionic core $(He+Na)^+$, the pseudopotential technique can be conveniently used to describe the molecular structure. We have used an $l$-dependent, Gaussian-type pseudopotential to represent the interaction between the Rydberg electron and each of the two cores. The form of the pseudopotential is

$$V_p(r)=V_p^{\mathrm{SR}}(r)+V_p^{\mathrm{LR}}(r)\ , \tag{1}$$

where the short- and long-range parts are given, respectively, by

$$V_p^{\mathrm{SR}}(r)=\sum_{l,m} A_l \exp(-\xi_l r^2)\,|\,Y_{l,m}\rangle\langle\,Y_{l,m}\,| \tag{2a}$$

and

$$V_p^{\mathrm{LR}}(r)=-\alpha_d/[2(r^2+d^2)^2]-\alpha_q/[2(r^2+d^2)^3]-Z_{\mathrm{eff}}/r\ . \tag{2b}$$

The $l$-dependent parameters $A_l$ and $\xi_l$ used above have been chosen to fit the spectroscopic data and are given by Bardsley[19] and Pascale[20] for Na and He, respectively. $Z_{\mathrm{eff}}$ is the net charge of the core seen by the electron at an infinite distance; $\alpha_d$, $\alpha_q$, and $d$ are the static dipole and the effective quadrupole polarizabilities, and the cutoff distance, respectively (see Refs. 19 and 20), and $r$ is the distance of the electron from the core.

Now, taking $\mathbf{r}_a$ and $\mathbf{r}_b$ as the position vectors of the Rydberg electron from the alkali ion core and helium atom, respectively, and $R$ as the internuclear separation, the one-electron Hamiltonian can be written as

$$H_{\mathrm{el}}=-\tfrac{1}{2}\nabla_{\mathbf{r}}^2+V_p(\mathbf{r}_a)+V_p(\mathbf{r}_b)+V_{\mathrm{CT}}(\mathbf{r}_b,\mathbf{R})+V_{\mathrm{CC}}(\mathbf{R})\ , \tag{3}$$

where $V_{\mathrm{CT}}$ and $V_{\mathrm{CC}}$ are the cross polarization and the core-core interaction terms, respectively. The cross polarization term $V_{\mathrm{CT}}$ accounts for the polarization of the He atom by both the valence electron and the alkali core whereas, the alkali-core-helium interaction is accounted for by the $R$-dependent term $V_{\mathrm{CC}}$. We have incorporated these terms in the present calculation in the same manner as has been done by Pascale[20] using the same set of parameters. Of course, the inclusion of these terms is essential to ensure the correct behavior of the adiabatic potential at large internuclear distances.

The resulting Schrödinger equation is given by

$$H_{\mathrm{el}}\Phi_n^{\mathrm{BO}}(\mathbf{r},\mathbf{R})=E_n(R)\Phi_n^{\mathrm{BO}}(\mathbf{r},\mathbf{R})\ , \tag{4}$$

where $\Phi_n^{BO}$ represent the Born-Oppenheimer adiabatic electronic wave functions. The latter are represented by a linear combination of the atomic orbitals (LCAO), each of which is made up of a combination of Slater-type orbitals (STO) centered on the alkali atom.[17]

Kimura *et al.*[17] have found that the use of the STO proposed by Stevens *et al.*[21] along with the pseudopotential of Bardsley[19] reproduces quite well the four lowest electronic levels of the alkali atom. These authors have found their calculations to be in good agreement with the *ab initio* results for a number of systems and the calculated equilibrium parameters $R_e$ and $D_e$ also agree well with other theoretical calculations (see Ref. 17). We have used the same set of STO in the present calculation; higher orbitals for Na have also been incorporated by suitably adjusting the positions of the nodes of the valence electron wave function expanded in STO, using the experimental quantum defects. These orbitals, used with the sodium pseudopotentials,[19,20] are found to give Na energies accurate to within 1% of the spectroscopic values.[22] We were unable to find other calculations on the molecular structures of $(Na^*+He)$ in the literature; thus, for the first time, adiabatic electronic energy curves are reported for He interacting with a low-lying Rydberg Na atom. We shall see that these are found to give an adequate description of the quenching collision dynamics. We note that the pseudopotential method becomes invalid at very small internuclear separations ($R<2a_0$), where core-core overlap becomes significant. However, this does not affect our results since the important couplings take place at relatively large $R$ values. This fact also permits another important simplification,[12] the representation of the relative motion of the colliding atoms by a classical rectilinear trajectory and the expression of the total time-dependent electronic wave function in terms of an ETF-modified molecular electronic basis set:

$$\Psi(\mathbf{r},t)=\sum_n a_n(t)\Phi_n^{BO}(\mathbf{r},R)F_n(\mathbf{r},R) \times\exp\left[-i\int E_n(R)dt+1/8V^2t\right], \quad (5)$$

where $F_n(\mathbf{r},R)$ represents the electron translation factors given as

$$F_n(\mathbf{r},R)=\exp[(i/2)f_n(\mathbf{r},R)\mathbf{r}\cdot\mathbf{V}] . \quad (6)$$

In the above expression, $V$ is the relative nuclear velocity $\mathbf{V}=d\mathbf{R}/dt$ and $f_n(\mathbf{r},R)$ represents the switching function. Since, in the present case, we have used a one-center LCAO expression for the adiabatic molecular wave function, the atomic form of the switching function is appropriate; this is equivalent to choosing $f_n$ to be $\pm1$ depending on the nucleus to which the electron is attached.

In order for the wave function in Eq. (5) to satisfy the time-dependent Schrödinger equation, the expansion coefficient must satisfy the standard set of coupled equations

$$i\dot{a}_n(t)=\sum_{k(\neq n)}\mathbf{V}\cdot(\mathbf{P}+\mathbf{A})_{kn}a_k\exp\left[-i\int^t(E_n-E_k)dt\right] . \quad (7)$$

where only the first-order terms in $V$ have been retained as appropriate for the present impact energy. In Eq. (7), $\mathbf{P}$ and $\mathbf{A}$ represent the nonadiabatic coupling matrix and its correction term, respectively. In the rotating frame (which rotates with the internuclear axis), the coupling $\mathbf{V}\cdot(\mathbf{P}+\mathbf{A})$ can be expressed as a sum of radial and angular terms, which at the low velocities considered here can be accurately calculated by considering only the first-order terms in the relative velocity (see Kimura *et al.*[17]).

The coupled equations (7) are solved for each contributed impact parameter and subject to the initial condition

$$a_k(-\infty)=\delta_{ik} , \quad (8)$$

where $i$ designates the initial state. Hence the probability for the transition to the $k$th state is given by

$$P_k(E,b)=|a_k(+\infty,b)|^2 , \quad (9)$$

and thus the corresponding cross section is

$$Q_k(E)=2\pi\int db\, bP_k(E,b) . \quad (10)$$

The range of impact parameters required in Eq. (10) depends on the radius of the Rydberg atom which is given by

$$r=\tfrac{1}{2}[3n^{*2}-l(l+1)] ,$$

where $n^*=n-\delta_l$ is the effective quantum number and $\delta_l$ is the quantum defect of $nl$ state. For example, in the case of Na(6$s$) ($n^*=n-\delta_0=4.65$; $r=32.4a_0$) colliding with ground-state He, impact parameters up to $25a_0$ were found to be adequate for calculating the cross sections; increasing the same even beyond $30a_0$ did not make any significant change in the calculated values. Here it may also be pointed out that the straight-line trajectories with $b\leq4a_0$ were found to make a negligible contribution to the calculated cross sections. It can, therefore, be safely concluded that the unphysical trajectories in the region of core-core overlap do not play any significant role in the present calculation.

## III. RESULTS AND DISCUSSION

State-changing cross sections have been calculated for Na atoms in low-lying Rydberg states, especially Na(6$s$) and Na(9$s$), colliding with ground-state He. We have examined the energy dependence of these cross sections and have carried out a number of two- and three-state calculations to confirm the mechanisms thought to be important. The objectives of carrying out a comparative study of Na(6$s$) and Na(9$s$) systems were to illustrate the different mechanisms that are involved in the two cases and also to examine the effects that the effective energy defects can have on the magnitude of the quenching cross sections.

### A. Adiabatic potentials and couplings

The probable mechanisms that control state changing can be understood by studying the molecular adiabatic potential curves. For the 14-state calculation, the curves are presented in Fig. 1, where 9$s$ $\Sigma$ represents the initial

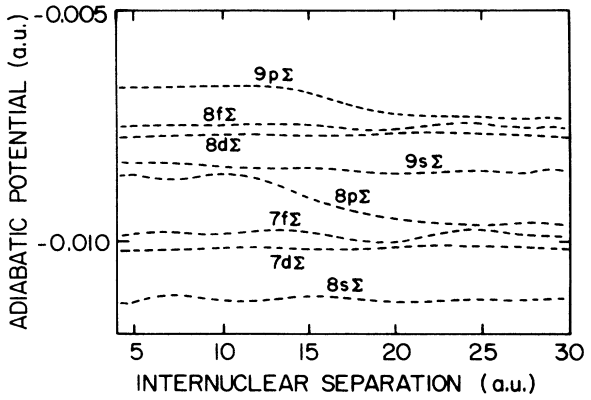


FIG. 1. Adiabatic potential curves of 14-state calculations for the Na($9s$)+He collision. The $8s$ Σ, $7d$ Σ, $7f$ Σ, $8p$ Σ, $9s$ Σ, $8d$ Σ, $8f$ Σ, and $9p$ Σ are Σ adiabatic states resulting from interaction of Na with ground-state He.

channel, which correlates with Na($9s$) interacting with ground-state He. The Π, Δ, and higher manifold states have been purposely left out of the figure so as to avoid confusion. However, in Fig. 2, the Σ and Π states that correlate with the $7f$, $8p$, $9s$, $8d$, and $8f$ states of Na interacting with ground-state He are presented.

In Fig. 1, it is apparent that $\Delta E(R)$ is very small, and the corresponding radial couplings very large, for the $9s$ Σ and $8p$ Σ curves around $R=11a_0$. There is also an avoided crossing between the $8p$ Σ and $7f$ Σ curves around $R=24a_0$ (see Fig. 2), which is manifested by strong radial coupling between these states, and near degeneracy with the $8p$ Π curve leading to strong angular couplings also in that region. The $7d$ Σ curve is very close to that of $7d$ Π, the two virtually merging together for $R>11a_0$ (not shown). Similarly the $7f$ Π curve lies closer to that of $7d$ Σ than for $7f$ Σ, both of which couple strongly to one another around $R=20a_0$. On the other hand, the $8p$ Π curve is found to be well separated from that of $8p$ Σ, except beyond $R=24a_0$. We also

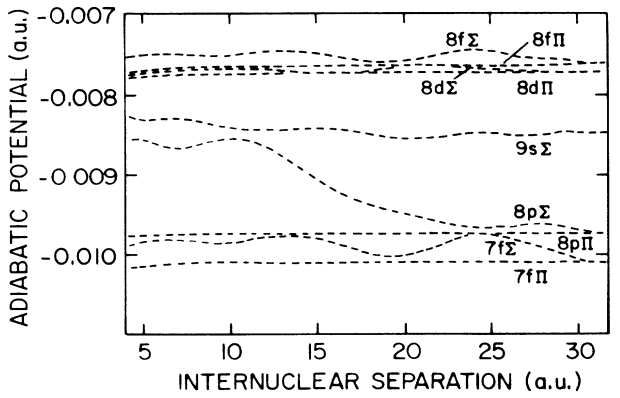


FIG. 2. Adiabatic potential curves of five Σ and four Π states for Na($9s$)+He collision. $7f$ Σ, $7f$ Π, $8p$ Σ, $8p$ Π, $9s$ Σ, $8d$ Σ, $8d$ Π, $8f$Σ, and $8f$ Π are different Σ and Π states resulting from collision of five different states of Na with ground-state He.

point out here that above the initial molecular state $9s$ Σ, the $8d$ Σ and $8f$ Σ curves possess an avoided crossing around $R=20a_0$. The $8d$ Π, $8f$ Π, and $8d$ Σ are nearly degenerate.

Selected radial coupling matrix elements, illustrated in Fig. 3, reflect the nature of the energy curves. For example, very strong radial coupling between $9s$ Σ and $8p$ Σ is observed around $R=11a_0$, as expected from the avoided curve crossing. Similarly, strong radial coupling between $8p$ Σ and $7f$ Σ is observed in the vicinity of $R=25a_0$. An avoided crossing between $7f$ Σ and $7d$ Σ around $R=20a_0$ results in strong radial coupling in the same region (not shown). Strong radial coupling between $8d$ Σ and $8f$ Σ around $R=20a_0$ also follows from the near crossing of the respective curves. In Fig. 4 selected angular coupling matrix elements relevant to the reaction are illustrated. Of particular importance is the strong angular coupling between $9s$ Σ and $8d$ Π for $R\leq 11a_0$ and that between $9s$ Σ and $8f$ Π over an extended range of $R$.

The relevant energy curves used in the close-coupling calculation for total depopulation of Na($6s$) are presented in Fig. 5 (for clarity only Σ states have been shown). As is expected, the energy curves corresponding to the smaller principal quantum number are energetically well separated from one another.

### B. Results for Na($9s$) state

In the thermal-energy region, the calculated deexcitation cross sections of Na($9s$) exhibit a small but significant energy dependence; they are found to decrease slowly with increasing impact velocity. This energy dependence is illustrated in Fig. 6 where, in addition to the total cross sections for depopulation of Na($9s$), contributions from both the Σ and Π final states are also presented. It should be noted that the basis sets used here are limited to only eight Σ ($m=0$) and six Π ($|m|=1$) states corresponding to all $s$, $p$, $d$, and $f$ atomic states between Na($8s$) and Na($9p$). Although higher-$m$ states can be populated through strong angular coupling within the nearly degenerate $n$ manifold, the rate of disappearance of the Na*($ns$) state (i.e., quench-

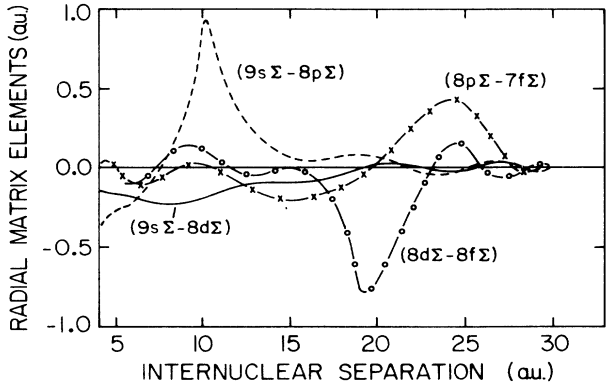


FIG. 3. Radial matrix elements for Na($9s$)+He collision. The radial matrices for $9s$ Σ→$8p$ Σ, $8p$ Σ→$7f$ Σ, $9s$ Σ→$8d$ Σ, and $8d$ Σ→$8f$ Σ transitions are labeled.

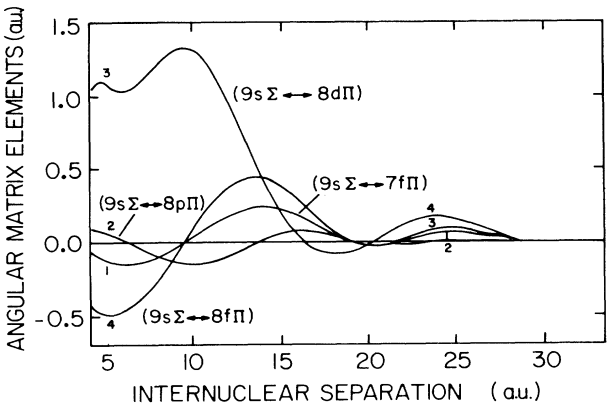


FIG. 4. Angular matrix elements for Na(9$s$)+He collision. The angular matrices for 9$s$ $\Sigma\leftrightarrow 7f$ $\Pi$, 9$s$ $\Sigma\leftrightarrow 8p$ $\Pi$, 9$s$ $\Sigma\leftrightarrow 8d$ $\Pi$, and 9$s$ $\Sigma\leftrightarrow 8f$ $\Pi$ transitions are labeled.

ing) is assumed not be be affected significantly by inclusion of $|m|\geq 2$ states. Some test studies using the limited basis with $|m|\leq 5$ have been carried out in order to assess the importance of high-$m$ states. In a test study including $7f$, $|m|=0,1,2$ and 3 with $7f$, $m=0$ chosen as the initial state it is found that the magnitudes of angular coupling matrix elements among these states are large and their $r$ dependence is long range. However, the flux does not flow primarily to higher-$m$ states. Only about 15% of the probability flux is transferred to states $|m|>2$ at large $R(>20a_0)$, i.e., in the outer part of the collision. Nevertheless, the final $m$ distribution resulting from the calculations reported in this paper is not expected to be accurate.

The cross section for excitation of Na(9$s$) to Na(8$p$) is dominated by the 9$s$ $\Sigma\rightarrow 8p$ $\Sigma$ transition at the avoided curve crossing. The contribution due to formation of 8$p$ $\Pi$ through angular coupling is very small. It is also observed that the $\Sigma$ cross section systematically decreases with increasing impact velocity in the energy range studies here. The strong radial coupling between the 9$s$ $\Sigma$ and 8$p$ $\Sigma$ states around $R=11a_0$ is mainly responsible for the transition. With an increase in impact energy, it

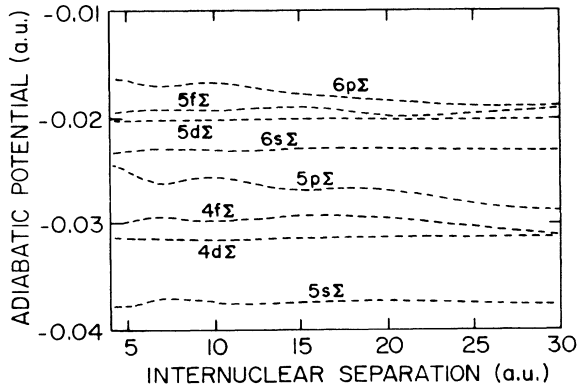


FIG. 5. Adiabatic potential curves of 14-state calculations for Na(6$s$)+He interaction. Labels are the same as in Fig. 1, except that different $s$, $p$, $d$, and $f$ states of Na lying between 5$s$ and 6$p$ have been used to construct these molecular states.

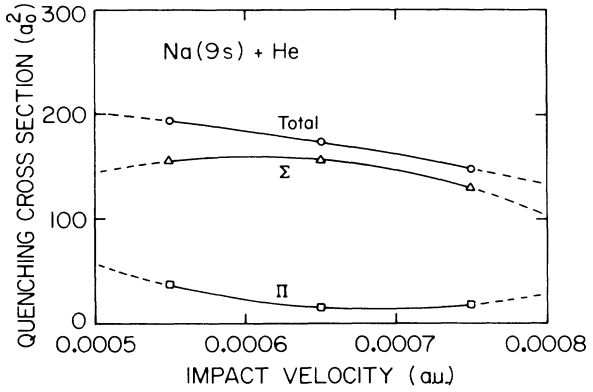


FIG. 6. Variation of cross sections with impact velocity for quenching of the 9$s$ state of Na colliding with He($1s^2$). △ and □ are the respective contributions due to formation of different $\Sigma$ and $\Pi$ states, and ○ is the total cross section. — — — is the extrapolation.

is expected that the transfer of flux at the avoided crossing will become increasingly diabatic, at such a large $R$ value, thereby resulting in a net decrease in the transition cross section. This behavior was confirmed by a two-state calculation

It is somewhat surprising that the cross section for the transition to Na(7$f$), as shown in Fig. 7, is found to be the largest in magnitude, even though the 7$f$ states is only the second closest state to 9$s$ in energy. Moreover, this cross section is found at first to increase with increasing impact velocity but then at higher relative energies to decrease again. The transition from Na(9$s$) to Na(7$f$) takes place in two steps. Strong radial coupling between 9$s$ $\Sigma$ and 8$p$ $\Sigma$ around $R=11a_0$ is responsible for the first transient step. Strong radial coupling (primarily diabatic in nature) between 8$p$ $\Sigma$ and 7$f$ $\Sigma$ in the vicinity of $R=25a_0$ strongly favors the final transition to the 7$f$ state. The absence of a similar strong coupling mechanism in the Na(6$s$)+He interaction (see Fig. 5) means that the majority of flux transferred from 6$s$ $\Sigma$ to 5$p$ $\Sigma$

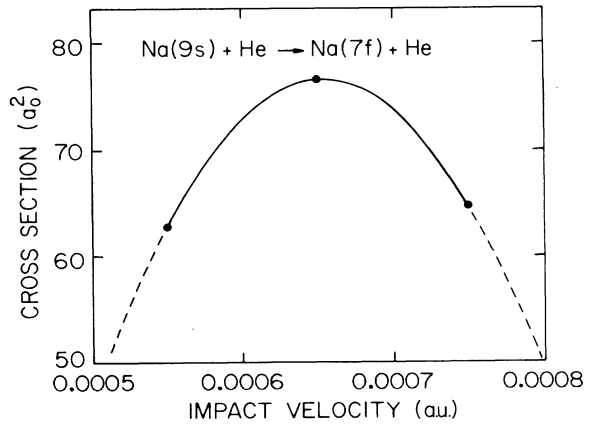


FIG. 7. Variation of cross sections with impact velocity, for transition to Na(7$f$) from Na(9$s$) colliding with He($1s^2$). Symbols are as in Fig. 6; contribution due to formation of the $\Pi$ state is negligibly small.

remains there permanently, thus ensuring that deexcitation to Na($5p$) is the dominant quenching transition. Returning to Na($9s$), we note that since the strong radial coupling controlling the second step ($8p\ \Sigma \rightarrow 7f\ \Sigma$) takes place at a relatively large value of $R$ and is primarily diabatic, one may expect that the crossing probability will approach unity with increasing impact energy. Two-state calculations have been carried out to confirm this behavior. The cross sections for the $9s\ \Sigma \rightarrow 7f\ \Sigma$ transition simply reflect the velocity dependence of the probability for the transition from $9s\ \Sigma$ to $8p\ \Sigma$ at higher velocities.

We have also investigated the time evolution of the collision probability in a number of five-state close-coupling calculations at different relative velocities and impact parameters. Representative calculated probabilities of transition from $9s\ \Sigma$ to the $8p\ \Sigma$ and $7f\ \Sigma$ states at impact velocity 0.000 75 a.u. and $b = 11a_0$ have been graphically presented in Fig. 8. Thus the evolution of the state amplitudes also supports the two-step mechanism which is responsible for populating both Na($7f$) and Na($8f$) from the parent Na($9s$).

Cross sections for transition to Na($7d$) and Na($8s$) are found to be small. Still, the transition to Na($7d$) is the only case where formation of the $7d\ \Pi$ state is found to be important.

Mechanisms important for upward transitions from Na($9s$) differ from those effective for downward transitions in that the $\Pi$ state contributes significantly to the total excitation cross sections from Na($9s$), and in certain cases may even be dominant. Once again, we find that the transition to the $f$ state ($8f$, in this case) has the largest cross section, although energetically it is Na($8d$) that lies closest in energy to Na($9s$). The total cross section for excitation of Na($8f$) is found to systematically decrease with increasing impact energy, while the contribution from the formation of the $8f\ \Sigma$ state remains nearly constant throughout the range investigated (see Fig. 9). At very low impact energy, formation of $8f\ \Pi$ is favored over that of $8f\ \Sigma$. However, as the impact velocity increases, the $8f\ \Sigma$ state becomes more important. We have performed a number of two-state calculations to confirm the two-step nature of the transition that leads to

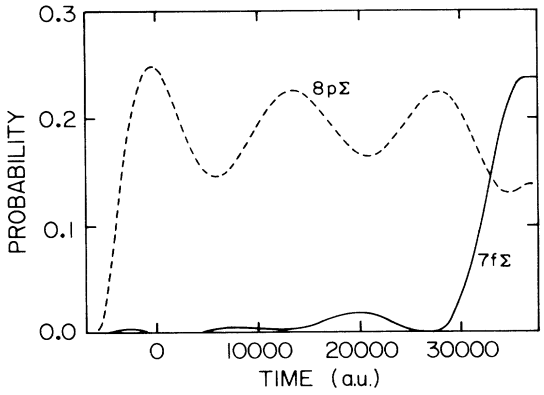


FIG. 8. Time evolution of collision probabilities at relative velocity 0.000 75 a.u. ($E = 1.383 \times 10^{-3}$). $8p\ \Sigma$ and $7f\ \Sigma$ represent the probabilities of transition from the $9s\ \Sigma$ state to the $8p\ \Sigma$ and $7f\ \Sigma$ states, respectively.

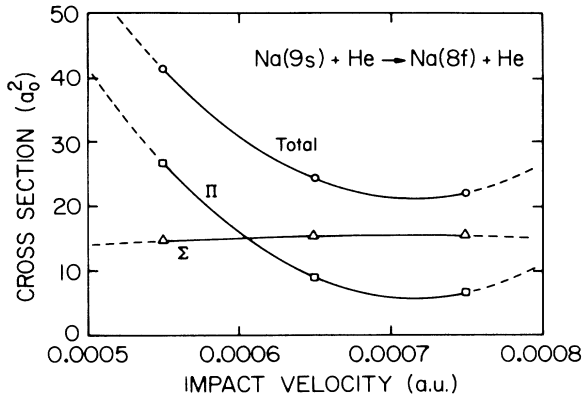


FIG. 9. Variation of cross sections with impact velocity for transition to the Na($8f$) state for Na($9s$) colliding with He($1s^2$). Symbols are as in Fig. 6.

the formation of Na($8f$). The energy dependence of the cross section for excitation to the next higher level, Na($8d$), is somewhat different. After an initial decrease, this cross section tends to increase with increasing impact velocity. The contributions of both $\Sigma$ and $\Pi$ states show roughly the same energy dependence and make about the same contributions to the cross section (Fig. 10; see also Fig. 11). Although the existence of very strong coupling between all four of the molecular states arising from Na($8d$) and Na($8f$) complicates the picture (as was the case with the $7d$ and $7f$ levels for the downward transitions), we can identify the most important mechanisms.

Returning again to Figs. 3 and 4, we can identify the important coupling matrix elements. There is a fairly strong radial coupling between the $9s\ \Sigma$ and $8d\ \Sigma$ states at smaller-$R$ values and strong angular couplings between the $9s\ \Sigma$ and $8d\ \Pi$ states around $R = 11a_0$. Thus significant flux transfer can occur from $9s\ \Sigma$ to $8d\ \Sigma$ and $8d\ \Pi$ at smaller-$R$ values, particularly if the relative collision velocity is not large. However, just as in the case of deexcitation, here also, the strong transition to Na($8d$) appears to be only a transient leading to excitation of Na($8f$). Since $8d\ \Sigma$ is strongly coupled to $8f\ \Sigma$ at large values of $R$ (see Fig. 3), most of the transferred flux is

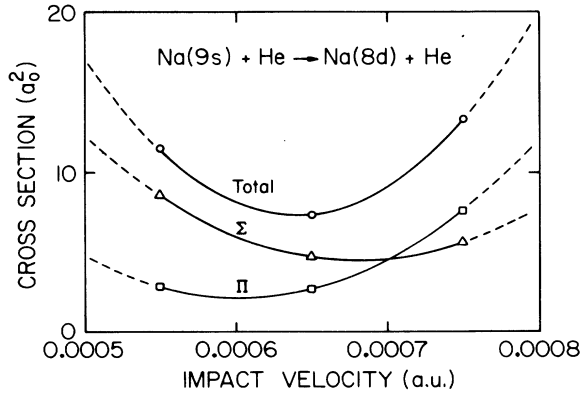


FIG. 10. Variation of cross sections with impact velocity for transition to the Na($8d$) state for Na($9s$) colliding with He($1s^2$). Symbols are as in Fig. 6.

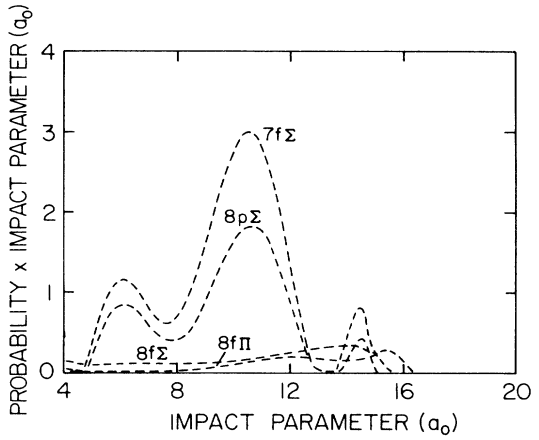


FIG. 11. Variation of the product of probability of transition $p$ and the impact parameter $b$ with $b$ at impact velocity 0.000 65 a.u. $7f$ Σ, $8p$ Σ, $8f$ Σ, and $8f$ Π represent transitions to the respective states from $9s$ Σ.

passed on to the next higher state, i.e., to $8f$ Σ. Moreover, the $8d$ Σ and $8f$ Π states are also strongly coupled throughout the region of interaction. Hence the second step of the two-step transition populates not only $8f$ Σ, but $8f$ Π as well. Fairly strong radial coupling between $8d$ Π and $8f$ Π at small-$R$ values (not shown in the figure) may also contribute to excitation of $8f$ Π. At low impact energy, because of the strong angular coupling between $8d$ Σ and $8f$ Π the latter state makes the larger relative contribution of the excitation to Na($8f$). However, with increasing energy, the radial coupling, which is strong at relatively large $R$ values, becomes more important so that the excitation of the Σ state dominates that of the Π state at higher velocities. Strong coupling between $8d$ Π and $8f$ Σ, at small-$R$ values also contributes, but leads to the same energy dependence. By performing several two- and three-state calculations we have confirmed these explanation of energy dependence as well as the two-step mechanism. The existence of comparatively weak, but still not completely negligible, coupling between the $9s$ Σ, $8f$ Σ, and $8f$ Π states may provide a small direct population of Na($8f$), especially at low impact velocities. We have determined through a test calculation that the inclusion of $10s$ or other more highly excited states of Na causes little change in the flux distribution as compared with the 14-state calculation.

It is important to note that the Na atomic states $nl$ ($l > 3$) are nearly degenerate with the $nf$ state. It is therefore possible that the probability flux transfer from the $8p$ molecular state to the $7f$ state proceeds to populate the higher-$l$ states. Similarly, a transition to the $8f$ state of Na may, in effect, represent population of the nearly degenerate $n$ manifold as well.

Although we do not show the results for excitation of Na($9p$), we find that it is mainly populated through the state $9p$ Σ; the contribution of the Π state is small but significant. The strong coupling between $8f$ Σ and $9p$ Σ at large-$R$ values, as well as an appreciable angular coupling between $8f$ Σ and $9p$ Π throughout the region, provide the mechanism for excitation of Na($9p$). The $9p$ Σ state is also populated through its strong angular coupling with $8f$ Π at large-$R$ values. The cross sections for excitation of Na($9p$) are found to decrease smoothly with increasing impact energy.

### C. Results for Na($6s$)

We have also carried out 14-state calculations to examine depopulation of Na($6s$) in a collision with He. The relevant adiabatic molecular states in this case are energetically well separated (see Fig. 5). Consequently, the effective energy defects for quenching of Na($6s$) and for various individual transitions are large in comparison with the cases previously discussed. The general features of the calculated cross sections are similar to those described for Na($9s$); however, there are differences in detail. The calculated cross sections for Na($6s$) are found to increase with increasing relative collision velocity, and the peak in the curve lies well beyond the range of thermal energies (see Fig. 12). Also in contrast to the Na($9s$) case is the overwhelming dominance of the deexcitation over excitation transitions at low impact velocities. This behavior simply reflects the larger effective energy defect for the upward transition (to $5d$ Σ) compared to that for a downward transition (to $5p$ Σ). It is only at the higher impact velocities that the cross sections for upward transitions begin to make significant contributions to the quenching of Na($6s$); this takes place through a two-step process in which the Na($5f$) is populated by strong radial coupling between $5d$ Σ and $5f$ Σ, around $R = 22a_0$. Direct transitions from Na($6s$) to Na($5f$) are highly improbable due to the weak radial and angular coupling between $6s$ Σ and $5f$ Σ and $5f$ Π, respectively.

### D. Comparisons with measurements and other theories

To the best of our knowledge there is only one set of experimental measurements for quenching of low-lying Rydberg levels of Na colliding with ground-state He, namely, those carried out by Gallagher and Cooke[4] at a temperature of 425 K for $6 \leq n \leq 11$, who have reported only the total depopulation cross sections for different $ns$

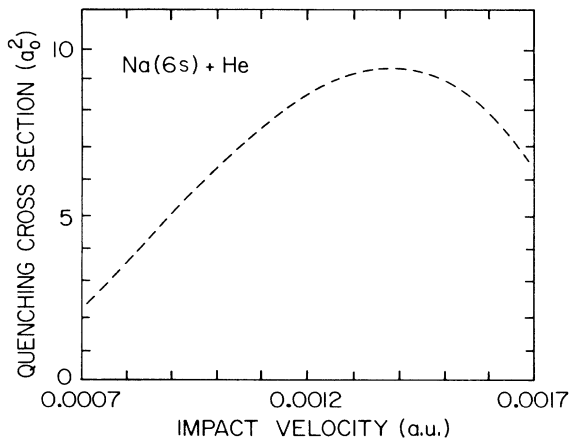


FIG. 12. Variation of cross section for total depopulation of Na($6s$) with impact velocity.

states of Na. These authors assumed the cross sections to be energy independent, in the investigated range, and derived the total cross sections from the measured rates by dividing by the mean Maxwellian velocity. However, our calculated cross sections are found to have some energy dependence, which we represent by a polynomial fit. Integration over the Maxwellian velocity distribution corresponding to $T=425$ K yields the rate constant (see Table I). The calculated quenching rate 0.0687 a.u. is about 3.5 times larger than the experimentally measured value $0.0193\pm0.0026$ a.u. for Na($9s$). In the case of Na($6s$) the calculate rate 0.003 25 a.u. and the experimentally measured[4] rate $0.001\,64\pm0.0004$ a.u. agree within a factor of 2.

It should be emphasized that for collision energies near the thresholds for excitation the semiclassical approach generally tends to overestimate the cross sections, particularly if a straight-line trajectory is used to described the relative motion of the interacting atoms. The threshold effect may be important since we are considering collision energies only a factor of 2 or 3 above threshold for excitation. However, the deexcitation cross sections, found to be particularly important for these systems, are expected to be less influenced by threshold effects. The use of a straight-line trajectory is justified by the relatively weak interaction potential associated with the initial channel in the cases studied.

As was mentioned earlier, Kaulakys[13] has calculated the total magnitude of the $n$-changing cross sections for Na($ns$)+He collisions in the thermal-energy region and has found agreement with the experimental measurements of Gallagher and Cooke[4] within the factor of 2. However, these calculations are based on the impulse approximation (IA), with the binary-encounter approximation used for the form factor. The reliability of this approach for low-lying excited states is definitely questionable (see Sato and Matsuzawa[8] and Petitjean and Gounand[9]). In these IA calculations the modified effective-range theory (MERT) of O'Malley[23] was used and the electron scattering length of the rare-gas atom (perturber) was used as an input parameter for calculating the state-changing cross sections. But the higher-order terms of the MERT expansion may not be negligible for low-lying states, especially for slow collisions.[8] Moreover, for such low-lying states, the use of the free-electron model is not justified; the full three-body interaction needs to be taken into account.[6] Similarly, Lebedev and Marchenko[12] have obtained analytical expressions for the total quenching cross section by using the Fermi pseudopotential method. They have presented results for the Na($ns$)+Ar collision showing an agreement to within a factor of 2 with the observations of Gallagher and Cooke.[4] However, since the Fermi model is not suitable for low-$n$ states, the agreement may well be fortuitous. In their model, the quenching of the $ns$ states of Na is largely due to the $ns\rightarrow n-1$, $l\geq 2$ transition. This represents excitation of the Na atom to energetically higher levels (see Figs. 1 and 2). However, for low-lying Rydberg states, the major contributions to the quenching cross section are observed to come from the downward transition (see Gallagher and Cooke[4].) It is only for higher principal quantum numbers that the upward transitions come into play.

TABLE I. Collision rate (in a.u.) for depopulation of Na($ns$) interacting with He at temperature 425 K.

| $ns$ state of Na | Calculated rate | Experimental rate[a] |
|---|---|---|
| $6s$ | 0.003 25 | $0.001\,64\pm0.0004$ |
| $9s$ | 0.068 | $0.019\,30\pm0.0026$ |

[a]Reference 4.

## IV. CONCLUDING REMARKS

The semiclassical impact-parameter method has been used to calculate the $n$-changing cross sections for collisions of low-lying Na($ns$) with He in the thermal-energy region. We have calculated not only the total magnitude of the quenching cross sections but have also examined the contributions of individual transitions. The energy dependence of the quenching process as well as the importance of the $R$-dependent energy defect for the reaction have also been investigated. We have also examined the most likely mechanisms responsible for the transitions by supplementing the large calculation with selected two- and three-state calculations.

It has been found that, for low-lying excited states, the parent level depopulates mainly through the process of deexcitation. These observations are in agreement with the experimental investigations of Gallagher and Cooke.[4] It is interesting to note that the dominance of deexcitation over excitation is contrary to what has been observed[8] in the case of highly excited Na($ns$) (see also Yoshizawa and Matsuzawa[24]). Matsuzawa and coworkers[8,24] have shown, using the impulse approximation, which is valid only for highly excited states, that cross sections to all final Na($nl$) channels other than $ns\rightarrow n-1$, $l>1$, are negligibly small. These authors have also pointed out that it is mainly the high angular momentum states, in such a reaction, that are dominantly populated in the final channels. These apparent differences between the results for low- and high-$n$ values is a direct consequence of the very small effective energy defects for quenching in the latter case. In spite of this difference, there is a similarity in that the major contribution to the quenching cross section comes from transitions (both excitation and deexcitation) to states $l>1$. Recalling that in the present case $l=3$ is degenerate with higher-$l$ levels of Na, we also find a propensity rule $\Delta l\geq 3$ for Na($9s$); cross sections for both excitation and deexcitation to the nearest $f$ levels are found to be the largest, at thermal-energy values.

While we believe that the mechanisms described here for quenching of Na($ns$) in collision with He are qualitatively correct, we still must emphasize that the magnitudes of the cross sections, particularly for individual transitions, are sensitive to changes in the potential

curves and coupling matrix elements. Thus we cannot be confident that our results are sufficiently accurate so as to place the experimental quenching rates in question. However, the essential collision dynamics discussed here remains unchanged since the flux escape mechanism to higher $l$ states and $m$ states is always expected to take place through the lower $l$ states and $m$ states that have been included and discussed in the present case.


## ACKNOWLEDGMENTS

Two of us (A.K. and N.F.L.) were supported in part by the U.S. Department of Energy, Office of Basic Energy Sciences, Division of Chemical Sciences, and the Robert A. Welch Foundation, and one of us (M.K.) was supported by the U.S. Department of Energy, Office of Health and Environment Research under Contract No. W-31-109-Eng-38.



*On leave from Department of Physics, D.A.V. College, Siwan 841 226, India.

[1]D. Kleppner, M. G. Littman, and M. L. Zimmerman, Sci. Am. **244**, 130 (1981).

[2]*Rydberg States of Atoms and Molecules,* edited by R. F. Stebbings and F. B. Dunning (Cambridge University Press, New York, 1983).

[3]E. Fermi, Nuovo Cimento **11**, 157 (1934).

[4]T. F. Gallagher and W. E. Cooke, Phys. Rev. A **19**, 2161 (1979).

[5]J. B. Delos, Rev. Mod. Phys. **53**, 287 (1981).

[6]E. de Prunele and J. Pascale, J. Phys. B **12**, 2511 (1979).

[7]*Reference Data on Atoms, Molecules, and Ions,* edited by A. A. Radzig and B. M. Smirnov (Springer-Verlag, Berlin, 1985).

[8]Y. Sato and M. Matsuzawa, Phys. Rev. A **31**, 1366 (1985).

[9]L. Petitjean and F. Gounand, Phys. Rev. A **30**, 2946 (1984).

[10]A. Omont, J. Phys. (Paris) **38**, 1343 (1977).

[11]J. Derouard and M. Lombardi, J. Phys. B **11**, 3875 (1978).

[12]V. S. Lebedev and V. S. Marchenko, Zh. Eksp. Teor. Fiz. **88**, 754 (1985) [Sov. Phys.—JETP **61**, 443 (1985)].

[13]B. Kaulakys, J. Phys. B **18**, L167 (1985).

[14]B. Kaulakys, Zh. Eksp. Teor. Fiz. **91**, 391 (1986) [Sov. Phys.—JETP **64**, 229 (1986)].

[15]D. R. Bates and R. McCarroll, Proc. R. Soc. London, Ser. A **245**, 175 (1958).

[16]M. Kimura and N. F. Lane (unpublished).

[17]M. Kimura, R. E. Olson, and J. Pascale, Phys. Rev. A **26**, 3113 (1982).

[18]P. Valiron, A. L. Roche, F. Masnou-Seeuws, and M. E. Dolan, J. Phys. B **17**, 2803 (1984).

[19]J. N. Bardsley, Case Stud. At. Phys. **4**, 299 (1974).

[20]J. Pascale, Phys. Rev. A **28**, 632 (1983).

[21]W. J. Stevens, A. M. Karo, and J. R. Hiskes, J. Chem. Phys. **74**, 3989 (1981).

[22]C. E. Moore, *Atomic Energy Levels,* Natl. Bur. Stand (U.S.) Circ. No. 467 (U.S. GPO, Washington, D.C., 1949), Vol. 1.

[23]T. F. O'Malley, Phys. Rev. **130**, 1020 (1963).

[24]T. Yoshizawa and M. Matsuzawa, J. Phys. Soc. Jpn. **54**, 918 (1985).